Depositional conditions and source of rare earth elements in carbonate strata of the Aptian-Albian Mural Formation, Pitaycachi section, northeastern Sonora, Mexico

Jayagopal Madhavaraju* and Carlos M. González-León

Estación Regional del Noroeste, Instituto de Geología, Universidad Nacional Autónoma de México, Blvd. Colosio y Madrid, 83000 Hermosillo, Sonora, Mexico.
**mj@geologia.unam.mx*

ABSTRACT

Major, trace and rare earth elements (REE) concentrations in limestone beds of the Canova and El Caloso members of the Mural Formation in the Cerro Caloso Pitaycachi area were measured to understand the depositional conditions and source of REE. Contents of SiO_2 and Al_2O_3 and concentrations of Zr, Y and Th are higher in the Canova member than in El Caloso member, whereas the content of CaO is comparable in both members. The sum of REE content however is low in both the Canova (10.4 ± 2.6, n=12) and El Caloso (3.4 ± 2.1, n=2) members. These values indicate that carbonate sedimentation of the Canova and El Caloso possess seawater-like shale-normalized REE+Y patterns with 1) light REE depletion (Nd_N/Yb_N = 0.74 ± 0.08, n=12; 0.58 ± 0.2, n=2; respectively), 2) both negative and positive Ce anomalies (Ce/Ce : 0.81–1.10, 0.94 ± 0.10, n=12; Ce/Ce* : 0.60 to 0.91, 0.76 ± 0.22, n=2; respectively), and 3) superchondritic Y/Ho ratio (33.5 ± 4.0, n=12; 40.4 ± 8, n=2; respectively). The observed variations in Ce contents and Ce anomalies in the studied samples resulted from detrital input and scavenging processes. The limestones show positive Mn* values (0.439 to 0.850) and low contents of U (~0.35–1.70 ppm) and authigenic U (0.31–1.57 ppm) suggesting that they were deposited under oxygen-rich environment. The REE+Y patterns of the Canova samples are identical to those of Late Devonian carbonate sediments whereas the El Caloso samples are comparable to Holocene reefal microbalite with slight light REE depletion. This suggests that the limestones from Canova and El Caloso members possibly retained their original seawater-like REE patterns. The observed variability in REE content and REE+Y pattern is due to the presence of minor amounts of detrital materials in some samples. The present study reveals that the limestones still retain their original seawater-like pattern, provided that shale contamination was least (<5%), and they serve as a seawater proxy.*

Key words: geochemistry, rare earth elements, oxic environment, Lower Cretaceous, Mexico.

RESUMEN

Las concentraciones de elementos mayores, traza y tierras raras (REE) en las capas de calizas de los miembros Canova y El Caloso de la Formación Mural en el noreste de Sonora pueden ser usadas para interpretar las condiciones de ambiente de depósito y la fuente de tierras raras de esta secuencia sedimentaria marina. Los contenidos de SiO_2 y Al_2O_3 y las concentraciones de Zr, Y y Th son mayores

Madhavaraju, J., González-León, C.M., 2012, Depositional conditions and source of rare earth elements in carbonate strata of the Aptian-Albian Mural Formation, Pitaycachi section, northeastern Sonora, Mexico: Revista Mexicana de Ciencias Geológicas, v. 29, núm. 2, p. 478-491.

en el miembro Canova que en El Caloso, el contenido de CaO es alto en ambos miembros, mientras que la ΣREE es baja en ambos miembros (Canova = 10.4 ± 2.6, n=12 y El Caloso = 3.4 ± 2.1, n=2). Estos valores indican que la sedimentación carbonatada en el Canova y El Caloso presenta patrones de REE+Y normalizados a lutita similares al del agua de mar, con 1) empobrecimiento de REE ligeras (Nd_N/Yb_N = 0.74 ± 0.08, n=12; 0.58 ± 0.2, n=2; respectivamente), 2) anomalías tanto negativas como positivas de Ce (Ce/Ce : 0.81 a 1.10, promedio 0.94 ± 0.10, n=12; Ce/Ce* : 0.60 a 0.91, prom. 0.76 ± 0.22, n=2; respectivamente), y 3) y relación Y/Ho supercondrítica (33.5 ± 4.0, n=12; 40.4 ± 8, n=2; respectivamente). Las variaciones observadas en el contenido y anomalías de Ce en las muestras estudiadas resultan de la aportación detrítica y de procesos de retrabajamiento del sedimento en el fondo marino. Las calizas muestran valores positivos de Mn* (0.439 a 0.850), contenidos bajos de U (~0.35–1.70 ppm) y U autigénico (0.31–1.57 ppm) que sugieren fueron depositadas en un ambiente oxigenado. Los patrones de REE+Y en las muestras del miembro Canova son idénticos a los de los carbonatos del Devónico Tardío mientras que las muestras de El Caloso presentan patrones parecidos a los de las microbialitas arrecifales del Holoceno con leve empobrecimiento en REE ligeras. Esto sugiere que las calizas estudiadas posiblemente preservan los patrones de REE originales del agua de mar. La variabilidad observada en el contenido de REE y en el patrón de REE+Y se debe a la presencia de cantidades menores de material detrítico en algunas muestras. El presente estudio revela que las calizas de los miembros estudiados preservan un patrón original parecido al del agua de mar y considerando que la contaminación de arcillas fue baja (<5%) sirven como un indicador proxy del agua de mar.*

Palabras clave: geoquímica, elementos de las tierras raras, ambiente oxidante, Cretácico inferior, México.

INTRODUCTION

The distribution of the rare earth elements (REE) in marine waters, sediments and carbonate rocks has been discussed by many workers (Piper, 1974; Klinkhammer *et al.*, 1983; De Baar *et al.*, 1988; Elderfield *et al.*, 1990; Madhavaraju and Ramasamy, 1999; Armstrong-Altrin *et al.,* 2003; Webb and Kamber, 2000; Nothdurft *et al.*, 2004; Madhavaraju and Lee, 2009; Madhavaraju *et al.,* 2010; Nagarajan *et al.,* 2011). The concentrations of REE in seawater are principally influenced by different input sources (*e.g.*, terrestrial input from continental weathering and hydrothermal) and scavenging processes related to depth, salinity and oxygen levels (Elderfield, 1988; Greaves *et al.,* 1999). The unique feature of the seawater REE pattern reveals the uniform trivalent behavior of the elements (except Ce and Eu that exhibit multiple valences) and estuarine and marine scavenging processes (Nothdurft *et al.,* 2004). The studies on Ce anomalies in ancient marine authigenic sediments serve as a potential tool for establishing paleoredox conditions in ancient oceans (Wright *et al.,* 1984, 1987; Liu *et al.,* 1988). The typical features of the shale-normalised marine REE patterns are: uniform light REE depletion, negative Ce anomaly, positive La anomaly and high Y/Ho ratios (*e.g.*, De Baar *et al.,* 1991; Bau and Dulski, 1996) and they are differentiated from signatures of detrital input (flat pattern) and hydrothermal input (positive Eu anomaly, enriched LREE and MREE).

The REE signatures in ancient marine environment provide information on secular variations in detrital materials and oxygenation conditions in the water column (*e.g.*, Holser, 1997; Kamber and Webb, 2001). In ancient carbonate rocks, REE proxies provide valuable information regarding the paleoceanography (Liu, *et al.,* 1988; Holser, 1997; Shields and Webb, 2004), marine and estuarine redox history (German and Elderfield, 1990; Bellanca *et al.,* 1997; Lawrence and Kamber, 2006) and issues relating to the biogenicity of marine precipitates (Webb and Kamber, 2000; Van Kranendonk *et al.,* 2003). In early studies, limestones have been considered as a poor choice for marine REE proxies because of their high REE concentration when compared with modern skeletal carbonate (*e.g.*, biominerals), which are interpreted as the result of diagenetic REE enrichment (*e.g.*, Shaw and Wasserburg, 1985). Later, Webb and Kamber (2000) showed that non-skeletal carbonates (microbialites) commonly incorporate REE in equilibrium with seawater with partition coefficients higher than the co-occurring skeletal materials. Nothdurft *et al.* (2004) distinguished the paleogeographically controlled REE patterns in microbialites that are reliable with formation in estuarine fringing reefs versus offshore, more open marine settings. The aims of our study are to document the REE characters in the limestones from Canova and El Caloso members of the Aptian-Albian Mural Formation to determine the influence of terrigenous materials on REE distribution in carbonate rocks and also to test the usefulness of REE geochemistry for paleogeographic and paleoceanographic reconstruction.

GEOLOGY AND STRATIGRAPHY

The sedimentary succession of the Lower Cretaceous Bisbee Group is exposed in the north-central part of Sonora, and shows similar stratigraphic characteristics and are correlatable with similar rocks exposed in the southern Arizona and New Mexico in the United States of America (Ransome,

1904; Cantu-Chapa, 1976; Bilodeau and Lindberg, 1983; Mack *et al.,* 1986; Dickinson *et al.,* 1989; Jacques-Ayala, 1995; Lawton *et al.*, 2004). The Bisbee Group mainly comprises sedimentary rocks with subordinate amounts of volcanic rocks of Late Jurassic to Early Cretaceous age (Lawton *et al.,* 2004), and its type area is located in southeastern Arizona. It has been divided into four distinct formations from bottom to top, Glance Conglomerate, Morita Formation, Mural Formation and Cintura Formation. The Glance Conglomerate is composed of cobble- to boulder-conglomerate interbedded with volcanic flows and tuffs, and represent syntectonic rift deposits (Bilodeau *et al.,* 1987).

The Morita and Cintura Formations consist of reddish brown siltstone and lenticular beds of arkose and feldspathic arenite (Dickinson *et al.,* 1986; Klute, 1991), deposited in fluvial environments. These two formations are difficult to differentiate based only on their lithological characters, and therefore the marine sedimentary strata (Mural Formation) deposited between them are considered key to understanding Lower Cretaceous stratigraphy and basin configuration in the area. The fossiliferous clastic and carbonate rocks of the Mural Formation represent a major marine transgression during Aptian-Albian (Scott, 1987) in the region of Sonora and Arizona.

The clastic and carbonate sedimentary succession of the Mural Formation is well exposed in a 300 km long transect which extends from Sierra El Chanate (westernmost part) to Cerro El Caloso Pitaycachi (northeasternmost outcrops) in northern Sonora (Figure 1) (González-León *et al.,* 2008). Studies of the Mural Formation recognized minor lateral facies changes from west to east which are depicted in its eight lithostratigraphic members (Lawton *et al.,* 2004; González-León *et al.,* 2008). Their facies characteristics suggest that the depositional environments varied from restricted shelf with deltaic and fluvial influence to open shelf with coral rudist buildups and offshore shelf environments. The Mural members are from base upwards i) Fronteras, ii) Rancho Bufalo, iii) Cerro La Ceja, iv) Tuape Shale, v) Los Coyotes, vi) Cerro La Puerta, vii) Cerro La Espina, and viii) Mesa Quemada. In the northeasternmost Sonora, however, a lateral facies change occurs among these members with members of the Mural Formation recognized by Warzeski (1983, 1987) in the locality of Sierra Anibacachi-Cerro Caloso Cabullona. Warzeski (1983, 1987) recognized the lower and upper Mural Formation of Ransome (1904) based on the correlation with southeastern Arizona. At the Cerro Caloso locality, he identified from base upwards the lower Mural Formation, and the upper Mural Formation composed by the Canova, El Caloso, La Aguja and Agua Prieta members. González-León *et al.* (2008) recognized that the Cerro La Ceja and Tuape Shale members represent lateral, shallow marine facies changes with the lower Mural Formation at the Cerro Caloso Cabullona locality, while the Fronteras and Rancho Bufalo are not exposed or wedge. Similarly,

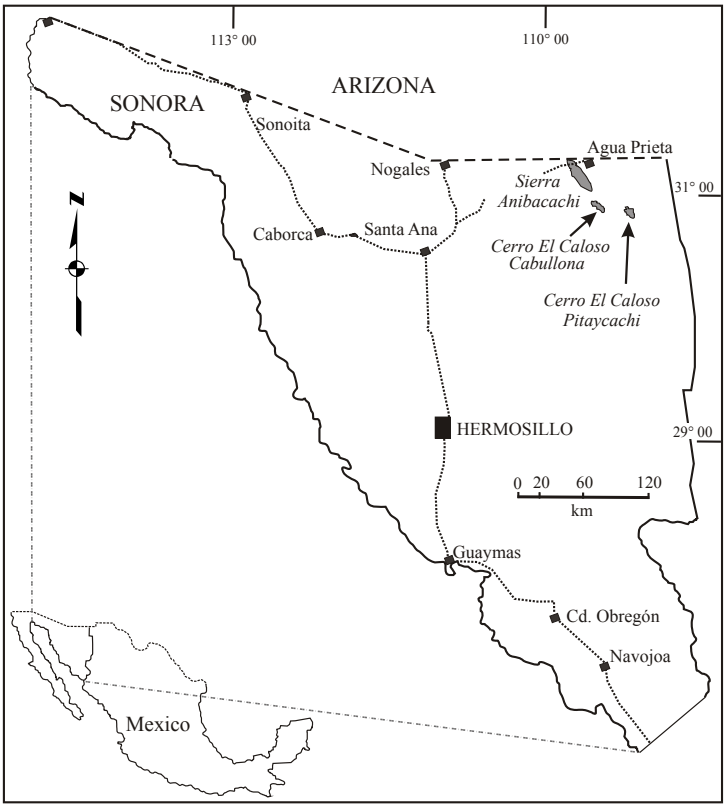

Figure 1. Location map of the studied sections of the Mural Formation.

González-León *et al.* (2008) correlated the Cerro La Puerta and Cerro La Espina members with the Canova, El Caloso, La Aguja and Agua Prieta members of that locality.

The stratigraphic section of the Mural Formation that crops out at Cerro Caloso Pitaycahi is located 30 km east of the Cerro Caloso Cabullona. The Canova member is 190 m thick and is composed of dark to light gray, thin to thick, massive to nodular beds of mudstone-wackestone forming shallowing- and thinning-up cycles. *Mesorbitolina texana* and other benthic foraminifera occur in its lower part, whereas pelagic foraminifera are present in its middle and upper parts, including *Colomiella tunisiana*, *C. Mexicana* Bonet, *Hedbergella delrioensis* (Carsey) and *Favusella washitensis* (González-León *et al.,* 2008). The El Caloso member is 26 m thick in this locality and represents only the lowermost part of this member. The maximum thickness of this member in Cerro Caloso Cabullona is 80 m (Warzeski, 1983). In the study section, this member is composed of medium-bedded bioclastic packstone, nodular, bioclastic packstone, medium to very thick bedded oolitic-oncolitic grainstone at the base. The upper part consists of medium to very thick beds of rudstone to calcarenite packstone-grainstone, and beds up to 2 m thick of coral boundstone. The Canova member in this locality represent deeper marine environments of deposition than their lateral correlative the Cerro La Puerta shale, whereas the El Caloso member that is correlative with the Cerro La Espina member represents a higher energy depositional environment with development of local coral reefs in a shallowing marine setting following deposition of the Canova member.

MATERIAL AND METHODS

The limestones from the Cerro El Caloso Pitaycachi section were selected for the present study (Figure 2). Fourteen samples were selected from the Cerro El Caloso Pitaycachi section for geochemical analyses and subsequently powdered in an agate mortar.

Major element composition was obtained by X-ray fluorescence in fused $LiBO_2/Li_2B_4O_7$ disks using a Siemens SRS-3000 X-ray fluorescence spectrometer with an Rh-anode X-ray tube as a radiation source. X-ray absorption/enhancement effects were corrected using the Lachance and Traill (1966) method, included in the SRS-3000 software. One gram of sample was heated to 1,000 ºC in porcelain crucibles for 1 hour to measure the loss on ignition (LOI). The geochemical standard JGB1 (GSJ) was used to determine data quality (Table 1). The analytical accuracy errors were better than ±2% for SiO_2, Fe_2O_3, CaO and TiO_2 (1.1%, 0.7%, 1.4%, 0.6, respectively) and better than ±5% for Al_2O_3, MgO, Na_2O and K_2O (3.3%, 3.6%, 4.2%, 4.2%, respectively). The accuracy errors of MnO and P_2O_5 were more than ±5% (5.3%, 7.1%, respectively).

Trace and rare earth elements were determined by an Agilent 7500 ce Inductively Coupled Plasma Mass Spectrometer (ICP-MS) according to standard analytical procedures suggested by Eggins *et al.* (1997). The geochemical standards IGLa-1, GSR2 and OU8 were used to monitor the analytical reproducibility (Table 2). The analytical results for the IGLa-1, GSR2 and OU8 obtained in the present study are compared with the published values (Table 2) reported by Govindaraju (1994) that allow to improve the quality and accuracy of the analysis. The analytical precision errors for Ba, Sc, Y, and Sr were

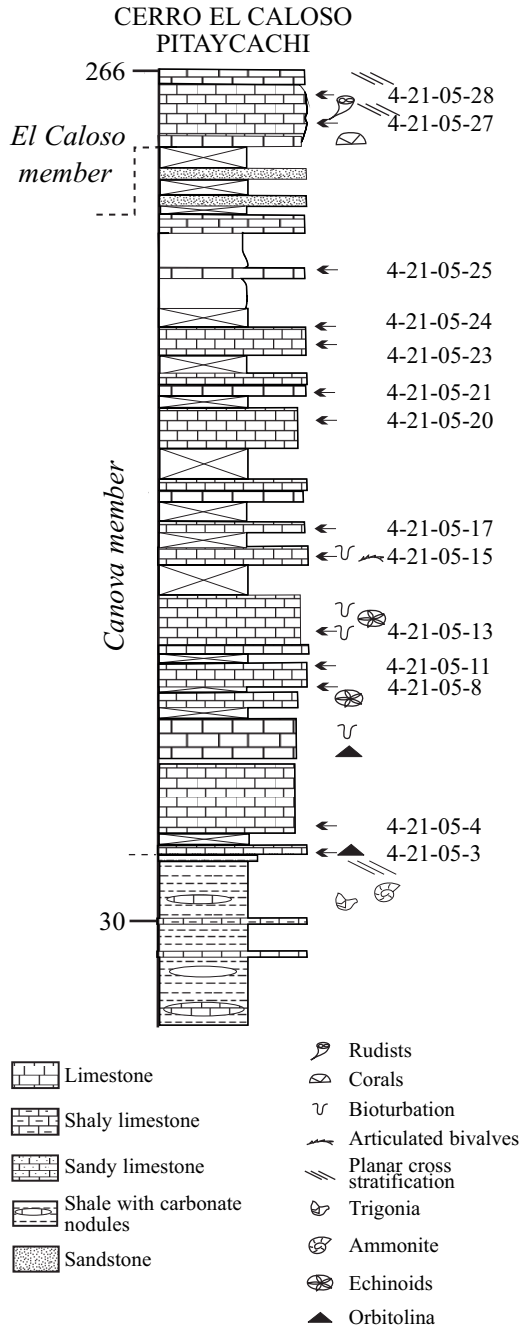

Figure 2. Lithostratigraphic section of the Mural Formation at Cerro El Caloso Pitaycachi (modified after González-León *et al.* 2008).

Table 1. Comparison of major oxide data for GSJ reference sample JBG1 with GSJ certificate of analysis data (Imai *et al.*, 1995) as well as limits of detection (LOD) data for XRF analyses.

Oxide	This study*	Literature value	LOD**
SiO_2	43.16	43.66	0.050
Al_2O_3	16.91	17.49	0.018
Fe_2O_3	15.16	15.06	0.006
CaO	11.73	11.90	0.040
MgO	7.57	7.85	0.015
K_2O	0.23	0.24	0.030
Na_2O	1.15	1.20	0.050
MnO	0.18	0.19	0.004
TiO_2	1.59	1.60	0.004
P_2O_5	0.06	0.056	0.004
LOI	-	-	-

* Major elements in wt. % are by XRF; ** LOD (limit of detection) in wt. %; - : not determined or not reported.

better than ±2%, for Cr, Zn, V, Zr, Nb and Rb were better than ±4%, while for Zn and Pb were better than ±6%. The analytical accuracy errors of certain trace elements (Cu, Ni, Th and U) were better than ±10%. The accuracy errors for rare earth elements such as Ce, Nd, Sm, Eu, Dy, Ho, Er and Yb were better than ±4%, and La and Pr were better than ±6%. The accuracies of Gd, Tb, Tm and Lu were better than ±10%. The detection limits for the instrument used in this study are given in Table 2. They generally obey the findings suggested by Verma *et al.* (2002), Santoyo and Verma (2003), and Verma and Santoyo (2005). Post-Archaean Australian Shale (PAAS) values (Taylor and McLennan, 1985) were used for REE-normalized diagrams. The anomalies in the PAAS-normalized REE patterns are expressed as Ce/Ce* = Ce/(2Pr-1Nd), Pr/Pr* = Pr/(0.5Ce+0.5Nd) and La/La* = La/(3Pr – 2Nd) (Bau and Dulski, 1996; Bolhar *et al.,* 2004).

The fourteen limestone samples were prepared for whole rock mineralogy following standard X-ray diffraction procedures (Biscaye, 1965; Muller, 1967; Grim, 1968;

Table 2. Comparison of trace and rare earth elements data for IGLa-1, GSR2 and OU8 reference samples.

Oxide/ Elements	IGLa-1	GSR2	OU8	This study*			LOD **
				IGLa-1	GSR2	OU8	
Ba	918.51	1020	528	917.57	1012.49	546.95	2.9712
Co	11.29	13.20	-	11.19	12.26	5.21	0.0213
Cr	29.21	33.40	21.50	28.63	32.16	22.17	2.4233
Cu	15.49	-	8.36	14.29	52.66	7.38	0.0290
Zn	78.75	71	-	75.90	66.24	8.08-	1.4882
Sc	12.19	9.50	3.63	11.99	9.63	29.61	0.0472
V	97.97	95.50	29.80	102.02	96.62	16.68	1.3595
Y	27.25	9.30	16	27.85	9.37	265.44	0.1902
Sr	574.75	790	264.40	562	803.60	-	6.0714
Zr	241.93	99	182.70	248.53	94.36	4.56	4.3175
Nb	18.96	6.80	4.46	19.5	6.03	10.66	0.0102
Ni	8.38	17	-	7.21	18.47	9.98	0.5802
Pb	10.24	11.30	9.64	19.90	10.70	68.14	0.3249
Rb	32.77	37.60	64.60	32.23	38.13	8.62	0.4833
Th	2.97	2.90	9.50	2.96	2.42	0.58	0.0151
U	0.99	0.90	0.74	1.01	0.83	13.80	0.0217
La	28.96	21.80	13.80	29.15	21.65	41.80	0.0136
Ce	56.73	40.00	41.80	58.31	40.58	3.12	0.0351
Pr	7.13	4.90	3.12	7.29	4.66	12.40	0.0088
Nd	28.65	19.00	12.40	29.59	18.26	2.42	0.0107
Sm	6.13	3.40	2.42	6.05	3.34	0.67	0.0918
Eu	1.85	1.02	0.67	1.79	1.10	2.32	0.0435
Gd	5.96	2.70	2.32	5.67	3.03	0.36	0.0028
Tb	0.88	0.41	0.36	0.89	0.38	2.26	0.0535
Dy	4.87	1.80	2.25	4.77	1.78	0.54	0.1087
Ho	0.99	0.34	0.51	1.04	0.33	1.57	0.0070
Er	2.76	0.85	1.59	2.69	0.84	0.26	0.0360
Tm	0.39	0.15	0.24	0.40	0.13	1.62	0.0071
Yb	2.60	0.89	1.66	2.55	0.77	0.24	0.0605
Lu	0.41	0.12	0.26	0.38	0.11	546.95	0.0077

* Trace and rare earth elements in ppm by ICP-MS. b ** LOD (limit of detection) in ppb. - not determined or not reported.

Table 3. Concentration of major oxides (wt%) in limestones of Canova and El Caloso members of the Mural Formation[1].

Member/ Sample No.	Clastic %	Carbonate %	SiO_2	Al_2O_3	Fe_2O_3	CaO	MgO	Na_2O	K_2O	TiO_2	P_2O_5	LOI	Total
El Caloso member													
4-21-05-28	1.6	98.4	0.5	0.25	0.22	54.8	0.66	0.06	0.03	0.02	0.03	43.3	99.87
4-21-05-27	3.9	96.1	1.3	0.37	0.37	52.9	1.94	0.02	0.06	0.01	0.02	42.7	99.69
Canova member													
4-21-05-25	9.1	90.9	5.6	1.11	0.76	50.4	1.26	0.03	0.14	0.04	0.03	40.1	99.47
4-21-05-24	6.0	94.0	4.3	0.46	0.43	52.3	0.74	0.06	0.10	0.03	0.02	41.4	99.84
4-21-05-23	6.3	93.7	4.2	0.75	0.48	52.1	0.95	0.07	0.07	0.03	0.03	41.2	99.88
4-21-05-21	7.6	92.4	4.7	1.07	0.40	50.8	1.42	0.05	0.13	0.03	0.03	41.1	99.73
4-21-05-20	8.4	91.6	4.7	1.66	0.49	50.9	1.15	0.09	0.25	0.06	0.03	40.5	99.83
4-21-05-17	10.2	90.8	5.3	1.24	0.46	50.4	1.31	0.10	0.21	0.05	0.04	40.6	99.71
4-21-05-15	6.8	93.2	3.2	1.02	0.64	51.8	1.36	0.14	0.09	0.03	0.03	41.4	99.71
4-21-05-13	5.0	95.0	3.0	0.62	0.42	52.5	0.96	0.20	0.05	0.02	0.03	42.1	99.90
4-21-05-11	6.7	93.3	3.8	0.80	0.47	52.0	1.20	0.19	0.08	0.03	0.03	41.0	99.60
4-21-05-8	7.8	92.2	4.0	1.25	0.56	51.6	1.29	0.11	0.21	0.05	0.03	40.9	100.00
4-21-05-4	6.3	93.7	3.4	1.16	0.53	51.9	1.00	0.20	0.15	0.04	0.03	41.4	99.81
4-21-05-3	7.4	92.6	4.8	1.07	0.58	51.2	1.01	0.25	0.12	0.03	0.03	40.8	99.89

[1] Reporting of significant figures follows the method of Verma (2005).

Hardy and Tucker, 1988). The powder samples were scanned from 2–70° (2θ) per minute. XRD was performed using a computer controlled Shimadzu Diffractometer system model 6000 with Cu kα radiation. The common minerals identified in these samples are quartz, feldspar and calcite. The clastic and carbonate percentages were calculated using the quartz, feldspar and calcite peaks in the X-ray diffractograms (Table 3).

RESULTS

Elemental variations

The major oxides concentrations of Canova and El Caloso members are given in Table 3. Contents of SiO_2 and Al_2O_3 are lower in the El Caloso samples (0.5 – 3.1%, 1.63 ± 1.33, n=2; 0.25 – 0.46%, 0.36 ± 0.11; respectively) than in the Canova samples (3.0 – 5.6%, 4.19 ± 0.81, n=13; 0.46 – 1.66%, 1.02 ± 0.31; respectively). Both the Canova and El Caloso samples show little variation in CaO contents (50.4 – 52.5% and 52.9 – 54.8%, respectively). Large variations in MgO contents are observed in the El Caloso samples (0.66 – 1.94%), whereas small variations are observed in the Canova samples (0.74 –1.42%). Fe_2O_3 content in all samples varies from 0.22 to 0.76%. The contents of Na_2O, K_2O, MnO, TiO_2 and P_2O_5 are very low in the limestone samples.

Common mineral phases that host high field strength elements (HFSE) such as Zr, Y and Th, are resistant to weathering when compared with phases hosting other trace elements (Taylor and McLennan, 1985). The limestones from the Canova member have higher concentrations of Zr, Y and Th than the El Caloso member (Table 4). The limestones of Canova and El Caloso members show low contents of Co, Sc and U. Large variations in Ba, V and Rb contents are found in the Canova samples whereas least variations are observed in the El Caloso samples. The Canova and El Caloso members exhibit least variations in Cu, Zn and Pb contents. Sr content of Canova and El Caloso members (449 – 677 ppm; 345 – 637 ppm; respectively) are slightly lower than the average value given for lithosphere carbonates (Sr = 610 ppm; Turekian and Wedepohl, 1961).

Concentrations of REE are generally lower in limestones than in shales, which suggest that the marine carbonate phases contain significantly less REE than terrigenous materials (Piper, 1974). Seawater contributes lower concentration of REE whereas the terrigenous sediments contain relatively high REE concentrations with non-seawater-like REE patterns (Nothdurft *et al.,* 2004). PAAS-normalized seawater-like REE patterns exhibit the following features: (1) significant light REE depletion, (2) negative Ce anomaly, and (3) slight positive La anomaly (*e.g.*, de Baar *et al.,* 1991; Bau and Dulski, 1996) and superchondritic Y/Ho ratios (*e.g.*, Bau, 1996). Total REE content is low in both Canova and El Caloso members (6.960 – 13.753 ppm, 10.4 ± 2.6, n=12; 1.929 – 4.954 ppm, 3.4 ± 2.1, n=2; respectively, Table 5). All limestones show shale-normalised seawater-like REE+Y patterns with (1) LREE depletion (Nd_N/Yb_N = 0.62 – 0.90, 0.74 ± 0.08, n=12; 0.45 – 0.71, 0.58 ± 0.18, n=2; respectively; Figures 3a-3c; Table 6), (2) both negative and positive Ce anomalies (Ce/Ce* : 0.63 – 0.98, 0.80 ± 0.11, n=12; 0.63 – 0.88, 0.76 ± 0.13, n=2; respectively; Figure 4; Table 6), (3) positive La anomalies (La/La*: 1.21 – 1.77, 1.46 ± 0.17, n=12; 0.95 – 1.10, 1.03 ± 0.11, n=2; respectively, Figure 4; Table 6), and (4). higher Y/Ho ratio (28.0 – 41.9, 33.5 ± 4.0, n=12; 34.5 – 46.3, 40.4 ± 8, n=2; respectively; Table 6).

Table 4. Concentration of trace elements (ppm) in limestones of Canova and El Caloso members of the Mural Formation[1]

Member/Sample No.	Mn	Ba	Co	Cu	Zn	Sc	V	Y	Sr	Zr	Ni	Pb	Rb	Th	U
El Caloso member															
4-21-05-28	155	0.04	1.12	2.08	14.5	0.12	4.9	1.11	637	2.53	6.60	1.29	0.52	0.09	0.63
4-21-05-27	248	1.5	1.28	2.10	13.7	0.31	3.4	1.55	345	3.04	6.50	1.95	2.23	0.12	0.35
Canova Member															
4-21-05-25	519	34	1.33	2.62	10.8	1.06	11.0	3.33	677	11.42	7.09	3.41	5.65	0.42	1.09
4-21-05-24	178	2.9	1.30	3.00	8.9	0.56	8.4	2.21	532	6.17	8.12	4.37	3.14	0.26	1.35
4-21-05-23	124	2.8	1.11	2.28	11.1	0.48	11.8	2.09	450	5.69	6.09	2.15	2.85	0.23	0.79
4-21-05-21	170	16.3	1.20	2.37	4.9	0.81	8.5	2.66	488	5.58	7.06	0.93	5.29	0.28	0.96
4-21-05-20	256	8.4	1.34	2.75	6.9	1.27	9.5	2.89	526	9.62	7.29	1.21	12.19	0.45	0.82
4-21-05-17	170	4.1	1.39	3.11	7.1	1.11	9.5	4.07	513	10.56	7.28	0.94	9.93	0.42	0.97
4-21-05-15	201	8.8	1.76	4.98	18.8	0.74	9.0	4.35	661	8.12	10.92	2.50	4.89	0.32	0.91
4-21-05-13	170	3.2	1.32	2.75	8.8	0.31	5.9	3.50	482	4.80	7.26	1.85	2.05	0.20	1.00
4-21-05-11	178	18	1.24	2.56	12.9	0.39	5.3	2.98	625	5.65	6.67	1.94	3.56	0.23	0.81
4-21-05-8	139	6	1.57	3.34	6.5	1.03	8.1	4.70	452	12.55	7.72	1.33	9.73	0.51	0.77
4-21-05-4	186	79	1.27	2.97	6.7	0.73	11.1	4.44	521	8.63	8.09	0.87	6.44	0.39	1.70
4-21-05-3	194	55	1.00	2.39	5.8	0.59	7.6	3.93	449	7.32	5.69	0.69	3.76	0.27	1.18

[1]Reporting of significant figures follows the method of Verma (2005).

DISCUSSION

Variations in Ce anomaly and depositional conditions

The Ce anomalies in marine carbonate rocks have been considered as suitable indicator for understanding contemporaneous paleo-redox conditions (Liu *et al.*, 1988). Many studies have been undertaken on Ce behaviour in marine phases to unravel paleoceanographic conditions (Grandjean *et al.,* 1987, 1988; Liu *et al.,* 1988; German and Elderfield, 1990; Nath *et al.,* 1997). As marine water shows negative Ce anomaly, similar Ce anomaly in limestones reveals the inclusion of REE directly from seawater or pore water under oxic condition. The deficiency of Ce relative to neighbouring rare earth elements is an important feature of modern seawater. This can be explained by oxidation of trivalent Ce to less soluble tetravalent Ce and successive removal by suspended particles through scavenging process (Sholkovitz *et al.,* 1994). However, Ce is remobilized and released into the water column in the suboxic environment resulting in a less negative to positive anomaly in seawater (De Baar 1991). But, the precise measurements of Ce anomalies in marine sediments may constrain redox conditions at the time and place of deposition (MacLeod and Irving, 1996).

La and Ce anomalies were calculated using the Ce/Ce* and Pr/Pr* ratios following the technique of Bau and Dulski (1996) (modified by Webb and Kamber, 2000). Most

Table 5. Concentration of rare earth elements (ppm) in limestones of Canova and El Caloso members of the Mural Formation.

Member/Sample No	La	Ce	Pr	Nd	Sm	Eu	Gd	Tb	Dy	Ho	Er	Tm	Yb	Lu	ΣREE
El Caloso member															
4-21-05-28	0.36	0.52	0.11	0.43	0.09	0.019	0.09	0.02	0.10	0.02	0.07	0.01	0.08	0.01	1.929
4-21-05-27	0.89	1.75	0.24	1.03	0.23	0.044	0.20	0.04	0.20	0.05	0.12	0.02	0.12	0.02	4.954
Canova Member															
4-21-05-25	2.53	5.25	0.61	2.65	0.57	0.113	0.53	0.10	0.52	0.12	0.31	0.04	0.24	0.04	13.623
4-21-05-24	1.43	2.48	0.35	1.47	0.31	0.063	0.29	0.06	0.29	0.07	0.18	0.03	0.17	0.03	7.223
4-21-05-23	1.48	2.84	0.36	1.62	0.35	0.064	0.31	0.06	0.31	0.07	0.19	0.03	0.17	0.03	7.854
4-21-05-21	1.62	3.00	0.40	1.75	0.40	0.075	0.38	0.08	0.41	0.09	0.26	0.04	0.22	0.03	8.755
4-21-05-20	2.08	4.10	0.51	2.23	0.48	0.091	0.45	0.09	0.46	0.10	0.28	0.04	0.24	0.04	11.191
4-21-05-17	2.65	4.01	0.58	2.48	0.51	0.103	0.51	0.10	0.51	0.12	0.33	0.05	0.27	0.04	12.261
4-21-05-15	2.51	3.74	0.57	2.47	0.53	0.105	0.51	0.10	0.53	0.12	0.32	0.04	0.27	0.04	11.855
4-21-05-13	1.69	2.07	0.34	1.56	0.33	0.070	0.35	0.07	0.38	0.09	0.24	0.04	0.21	0.03	7.470
4-21-05-11	1.64	2.09	0.32	1.40	0.28	0.060	0.30	0.06	0.30	0.07	0.20	0.03	0.18	0.03	6.960
4-21-05-8	2.75	4.53	0.64	2.85	0.60	0.123	0.60	0.12	0.61	0.14	0.38	0.05	0.31	0.05	13.753
4-21-05-4	2.69	3.74	0.56	2.49	0.54	0.110	0.54	0.11	0.57	0.13	0.36	0.05	0.30	0.04	12.230
4-21-05-3	2.25	3.94	0.53	2.38	0.53	0.110	0.54	0.10	0.55	0.12	0.33	0.04	0.25	0.04	11.710

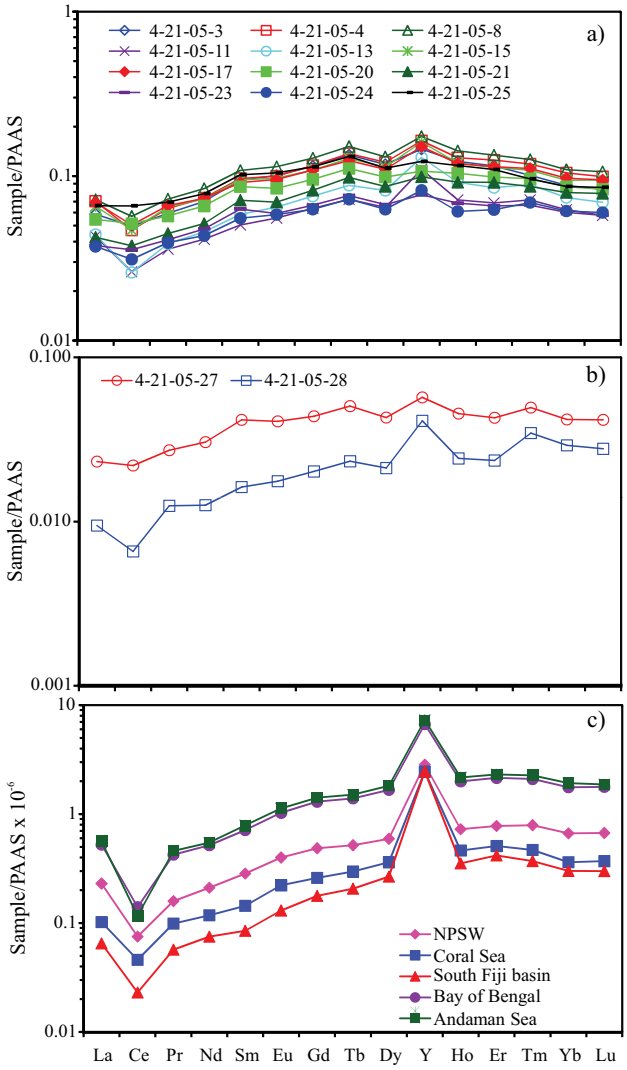

Figure 3. a) PAAS-normalized REE patterns of limestones of the Canova Member. b) REE patterns of the El Caloso Member. c) PAAS normalized REE patterns of modern seawater (NPSW: North Pacific shallow water, Sagami trough (Alibio and Nozaki, 1999), Coral Sea: South Pacific shallow seawater (Zhang and Nozaki, 1996), South Fiji Basin: Station SA12 (Zhang and Nozaki, 1996), Bay of Bengal: shallow water (Nozaki and Alibio, 2003) and Andaman Sea: shallow water (Nozaki and Alibio, 2003).

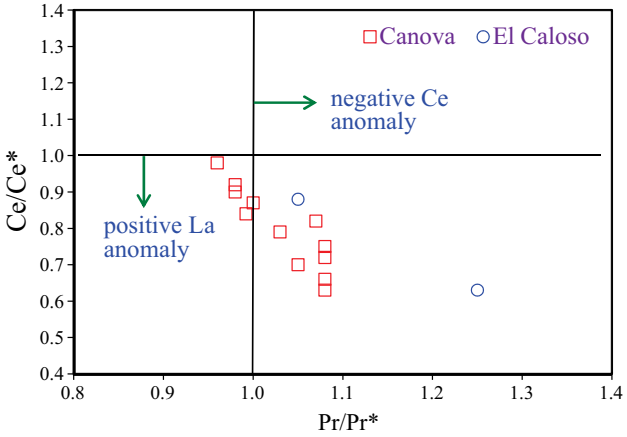

Figure 4. PAAS-normalized Ce/Ce* *vs.* Pr/Pr* plot to evaluate the La and Ce anomalies using the method of Bau and Dulski (1996) (as modified by Webb and Kamber, 2000) for limestones of Canova and El Caloso members of Mural Formation.

of the samples show negative Ce and positive La anomalies, whereas few samples exhibit absence of negative Ce anomalies (Figure 4). Ce/Ce* ratio is a function of the relative proportions of a pure seawater precipitate and clastic contamination, as well as REE concentrations of these two end members. With increasing clastic contamination the Ce/Ce* ratio approaches 1. The depletion of Ce relative to neighbouring REE is one of the characteristic features of seawater and marine carbonates deposited in the deep sea regions, and is due to the adsorption of Ce onto Fe-Mn particle surfaces by oxidation of Ce(III) to Ce(IV). In seawater, Ce/Ce^* values range from < 0.1 to 0.4 (Elderfield and Greaves, 1982; Piepgras and Jacobsen, 1992). Nine limestone samples show negative Ce anomalies (Figure 4), whereas few limestones show positive Ce anomalies. Positive Ce anomalies mainly occur due to detrital input (Nath *et al.,* 1997; Madhavaraju and Ramasamy, 1999; Madhavaraju and Lee, 2009; Madhavaraju *et al.,* 2010), diagenesis (Armstrong-Altrin *et al.,* 2003), scavenging process (Masuzawa and Koyama, 1989) and paleo-redox conditions (Liu *et al.,* 1988).

Deep marine environments with well developed oxic water columns, low sedimentation rates and active scavenging processes may favour coprecipitation of Ce(OH) on Fe-Mg coatings of sedimentary particles. The REE patterns having distinct positive Ce anomaly in settling particles strongly support the scavenging of Ce over remaining rare earth elements (Masuzawa and Koyama, 1989). In the present study, the Ce/Ce^* values have positive correlation with scavenging-type particle reactive elements (*e.g.*, Ce/Ce* *vs.* Mn, r=0.55; Ce/Ce* *vs.* Fe, r=0.42). The Canova member represents moderately deep to deep shelf marine environments whereas the El Caloso member represents a higher energy shallowing marine depositional environment (Warzeski, 1983). In some cases, Ce distribution may be linked to the redox cycling of Mn and/or Fe. The observed variations in Ce anomalies whether influenced by scavenging processes or paleo-redox changes can be tested using other redox sensitive elements (*e.g.*, Mn* values, contents of uranium and authigenic uranium).

The variations in the solubility of Fe and Mn may lead to remarkable fractionation of these metals across the redox boundaries. Most of the iron are fixed in sulphide under low *Eh* conditions, whereas manganese is incorporated under oxygenated conditions above the redox boundary (Krauskopf, 1979; Bellanca *et al.*, 1996). Machhour *et al.* (1994) and Bellanca *et al.* (1996) proposed the relationship Mn* using Fe and Mn concentrations [$Mn^* = \log[(Mn_{sample}/$

Table 6. Elemental ratios and anomalies in limestones of Canova and El Caloso members of the Mural Formation.

Member/Sample No	Ce/Ce*	La/La*	Pr/Pr*	La_N/Yb_N	Nd_N/Yb_N	Dy_N/Yb_N	Y/Ho	Mn*	Authigenic U (ppm)
El Caloso member									
4-21-05-28	0.63	0.95	1.250	0.31	0.45	0.73	46.3	0.845	0.60
4-21-05-27	0.88	1.10	1.050	0.55	0.71	1.03	34.5	0.795	0.31
Canova Member									
4-21-05-25	0.98	1.30	0.960	0.76	0.90	1.29	28.9	0.850	0.95
4-21-05-24	0.82	1.21	1.070	0.61	0.70	1.02	34.0	0.554	1.26
4-21-05-23	0.90	1.40	0.980	0.63	0.80	1.11	30.8	0.506	0.71
4-21-05-21	0.87	1.37	1.000	0.53	0.66	1.09	29.2	0.585	0.87
4-21-05-20	0.92	1.40	0.980	0.64	0.77	1.15	28.0	0.673	0.67
4-21-05-17	0.75	1.33	1.080	0.71	0.75	1.13	34.5	0.524	0.83
4-21-05-15	0.72	1.34	1.080	0.70	0.78	1.20	35.5	0.557	0.81
4-21-05-13	0.63	1.77	1.080	0.59	0.62	1.10	38.4	0.564	0.93
4-21-05-11	0.66	1.65	1.080	0.69	0.66	1.03	41.9	0.515	0.73
4-21-05-8	0.79	1.50	1.030	0.66	0.77	1.20	33.3	0.439	0.60
4-21-05-4	0.70	1.60	1.050	0.67	0.70	1.16	34.7	0.463	1.57
4-21-05-3	0.84	1.59	0.992	0.67	0.80	1.34	32.2	0.600	1.09

Mn_{shale})/(Fe_{sample}/Fe_{shale})] to understand the redox potential of the depositional environment. The values used for Mn_{shale} and Fe_{shale} to calculate Mn* are 600 ppm and 46,150 ppm, respectively (Wedepohl, 1978). The limestones of Canova and El Caloso members show significant positive Mn* values (0.439 – 0.850 and 0.795 – 0.845, respectively; Table 6). The significant positive Mn* values suggest that the limestones of this study were deposited under oxic condition.

Like Ce, Uranium is mainly fractionated from thorium in near surface environment (Whittaker and Kyser, 1993). Uranium is mobilized as U^{+6} in oxic environment and precipitated as U^{+4} in reducing environments (Anderson *et al.,* 1983; Nozaki *et al.,* 1981; Wright *et al.,* 1984). The limestones of both Canova and El Caloso members show low content of U (0.77 – 1.70 ppm and 0.35 – 0.63 ppm, respectively). The sediments deposited in oxygenated marine environment generally show low contents of U (Somayajulu *et al.,* 1994; Madhavaraju and Ramasamy, 1999), whereas high U contents are generally found in sediments from the oxygen minimum zone (Barnes and Cochran, 1990; Klinkhammer and Palmer, 1991; Sarkar *et al.,* 1993; Somayajulu *et al.,*1994; Nath *et al.,* 1997). The low content of U in Canova and El Caloso members are due to the mobilization of U^{+6} from sediments to water column under oxic environments. In addition, the concentration of authigenic uranium (authigenic U = Total U - Th/3) has also been used to understand the redox changes in the marine environments (Wignall and Myers, 1988). The authigenic U concentration below 2 suggest oxic conditions of deposition, whereas values above 2 indicate dysoxic conditions (Wignall and Myer, 1988). The limestones of this study show low authigenic U content (0.60–1.57 ppm, 0.31–0.60 ppm, respectively), which indicate that these limestones were deposited under an oxic environment. In addition, Ce/Ce* values show no correlation with Mn* values (r=-0.06, which suggests that the variation in Ce anomalies were not induced by the redox conditions.

The Ce/Ce* values show positive correlation with Al_2O_3, Th and Zr (r=0.58; 0.51; 0.49; respectively), whereas Ce shows significant positive correlations with Al_2O_3, Th and Zr (r= 0.84; 0.90; 0.93; respectively). The positive correlation of Ce and Ce/Ce* ratios with Al_2O_3, Th and Zr suggest that the variation in Ce and Ce anomalies in these limestones have been controlled by the detrital input.

Hence, the observed variations in Ce contents and Ce anomalies in the limestones of Canova and El Caloso members may be due to the influence of detrital materials. Furthermore, the Ce/Ce* values have positive correlation with scavenging-type particle reactive elements (Fe and Mn) which indicates that the variations in Ce anomalies might be related to scavenging processes.

Source of REE in marine limestones

The Canova and El Caloso limestones possess seawater-like REE+Y patterns. However, some variation exists among the LREE depletion, ΣREE contents, Y/Ho ratios, size of the La and Ce anomalies (Table 6). For both the Canova and El Caloso samples, ΣREE contents show positive correlation with Al_2O_3 (r= 0.85, n=14). In addition, the samples show positive correlation between Nd_N/Yb_N and Al_2O_3 (r= 0.59, n=14). These relationships suggest some detrital influence on sample REE contents. Seawater signatures in carbonate rocks may be effectively masked by detrital contaminations due to the higher REE concentration in detrital material and the generally flat REE pattern typical of common detrital materials (German and Elderfield, 1990; Bau and Dulski, 1996; Byrne *et al.,* 1996; Madhavaraju and

Ramasamy, 1999; Webb and Kamber, 2000; Madhavaraju and Lee, 2009; Madhavaraju *et al.,* 2010).

One limestone sample (4-21-05-28) from the El Caloso member has a comparatively low ΣREE content (1.929 ppm) and LREE depletion within the range of modern seawater (Nd_N/Yb_N = 0.45; modern shallow water = 0.205 to 0.492 for 50 m water depth; Zhang and Nozaki, 1996; de Baar *et al.*, 1985). The degree to which the detrital content affects the REE patterns in the Canova and El Caloso members can be tested assuming conservative mixing of PAAS and the low ΣREE limestone sample (4-21-05-28). The limestone sample 4-21-05-28 can be considered as the least contaminated by clastic input and used as a seawater-like end-member because it has low ΣREE content, significant depletion of LREE, REE pattern similar to modern seawater and superchondritic Y/Ho ratio. The REE concentration is high in shale and the inclusion of as little as 1 to 2% of fine grained material may significantly alter the Ce anomalies, LREE depletion and REE patterns (Nothdurft *et al.,* 2004). Shale samples from the Mural Formation (Madhavaraju *et al.*, 2008) show slight LREE depletion relative to PAAS. Conservative mixing of 4-21-05-28 with various proportions (1%, 2%, 5%, 10%, 20% and 50%) of both local shale (shale samples from Mural Formation, average of 25 samples) and PAAS (Table 7) illustrates the amount of shale contamination required to alter the seawater-like REE patterns in the limestones of Mural Formation (Figure 5). The well-developed seawater-like REE pattern of limestone sample 4-21-05-28 is maintained with up to 5% of REE contributed from the local shale, but the degree of LREE depletion decreases gradually. Due to its relatively higher ΣREE, a 2% contamination with PAAS effectively overprints the limestone seawater REE patterns (Nothdurft *et al.*, 2004). Considering the differences in REE distribution between local shale and PAAS, particularly with regard to the LREE, we suggest that the local shale concentrations instead of using PAAS values should be taken for calculating the percentage of detrital contamination present in the limestone samples.

The limestones show slight variations in La_N/Yb_N ratios (Table 6). The La_N/Yb_N ratios of these limestones are significantly lower than the values proposed by Condie (1991; about 1.0) and Sholkovitz (1990; about 1.3) for terrigenous materials. Thus, the studied limestones were less contaminated by terrigenous materials and the La_N/Yb_N ratios found in the present study are more or less similar to the Devonian carbonate sediments, Permian Limestone and Albian-Cenomanian Limestone and higher than the Holocene reefal microbialite (Table 8). The limestones of Canova and El Caloso members of the Mural Formation show seawater-like REE+Y pattern with enrichment of HREE relative to LREE and are compared with limestones yielding identical REE patterns to modern seawater (Figure 6; Late Devonian carbonate sediments, Nothdurft *et al.,* 2004; Permian Limestone, Kawabe *et al.,* 1991; Albian-Cenomanian Limestone, Bellanca *et al.,* 1997; Holocene

Table 7. The limestone of Canova Member (4-21-05-28), PAAS values and average Mural Shale values used for mixing calculations.

Elements	4-21-05-28		Average Mural Shale (n=25)[1]		PAAS
	ppm	N*	ppm	N*	ppm
La	0.36	0.009	25.55	0.661	38.2
Ce	0.52	0.007	53.00	0.666	79.6
Pr	0.11	0.012	5.93	0.672	8.83
Nd	0.43	0.013	25.77	0.760	33.9
Sm	0.09	0.016	5.23	0.942	5.55
Eu	0.019	0.018	1.00	0.926	1.08
Gd	0.09	0.019	4.63	0.994	4.66
Tb	0.02	0.026	0.89	1.150	0.774
Dy	0.10	0.021	4.70	1.009	4.66
Y	1.11	0.041	24.07	0.891	27.0
Ho	0.02	0.020	1.03	1.039	0.991
Er	0.07	0.025	2.86	1.004	2.85
Tm	0.01	0.025	0.37	0.914	0.405
Yb	0.08	0.028	2.41	0.855	2.82
Lu	0.01	0.023	0.37	0.855	0.433

[1]Madhavaraju *et al.*, 2008; N*: PAAS normalized values.

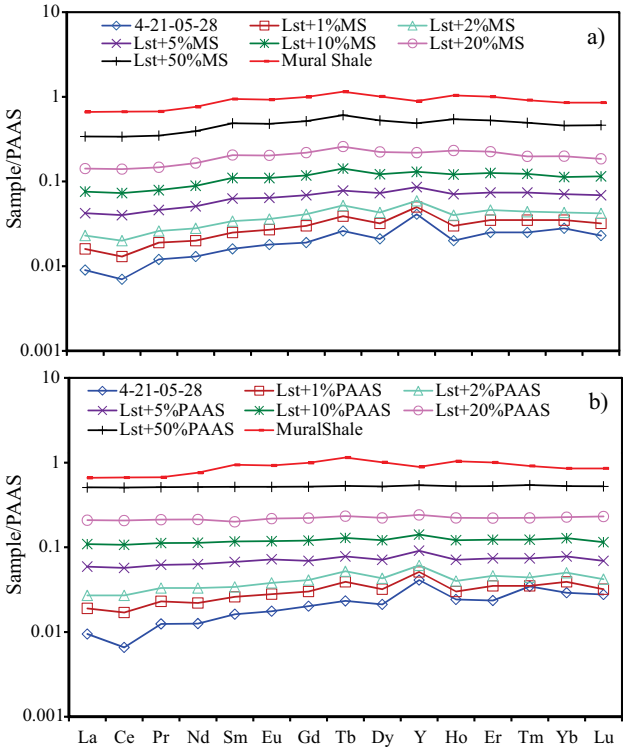

Figure 5. a) PAAS-normalized REE+Y pattern of the limestone of El Caloso Member (4-21-05-28) and idealized mixtures (1%, 2%, 5%, 10%, 20%, 50%) with average shale of the Mural Formation. It illustrates that the seawater pattern is retained upto 5% of shale contamination. b) PAAS-normalized REE+Y pattern of the limestone of El Caloso member (4-21-05-28) and hypothetical mixtures (1%, 2%, 5%, 10%, 20%, 50%) with PAAS. In this case minor contamination (<2%) significantly alters the seawater patterns. The PAAS- normalized REE+Y pattern of the Mural shale shows a slight LREE depletion.

Table 8. Average geochemical values of the Canova and El Caloso members compared to the carbonate rocks showing seawater-like REE patterns.

	Mural Formation			Late Devonian Cabonate Sediments[2]	Permian Limestone[3]	Albian-Cenomanian Limestone[4]	Holocene Reefal Microbialite[5]
	Canova Member[1a]	El Caloso Member[1b]	Average[1c]				
Ce/Ce*	0.94 ± 0.10	0.76 ± 0.22	0.91 ± 0.13	0.75 ± 0.05	0.24 ± 0.04	0.43 ± 0.09	0.74 ± 0.02
La_N/Yb_N	0.66 ± 0.06	0.43 ± 0.17	0.62 ± 0.11	0.73 ± 0.10	0.53 ± 0.34	0.84 ± 0.08	0.20 ± 0.02
ΣREE	10.4 ± 2.6	3.4 ± 2.1	9.4 ± 3.5	6.8 ± 4	3.2 ± 2.4	28.5 ± 10.7	0.96 ± 0.21
CaO	51.5 ± 0.4	54 ± 1.3	52 ± 1.2	-	-	-	-
Nd_N/Yb_N	0.74 ± 0.08	0.58 ± 0.2	0.73 ± 0.06	0.65 ± 0.11	0.34 ± 0.13	0.57 ± 0.10	0.25 ± 0.02
Dy_N/Yb_N	1.15 ± 0.09	0.88 ± 0.2	1.11 ± 0.3	0.42 ± 0.08	1.06 ± 0.05	0.89 ± 0.12	0.78 ± 0.04
Y/Ho	33.5 ± 4	40.4 ± 8.3	34.5 ± 5	40 ± 3.4	72 ± 12	44	56 ± 3

[1a,b,c]Present study, n=12, n=2, n=14, respectively; [2]Nothdurft *et al.*, 2004, n=7; [3]Kawabe *et al.*, 1991, n=2; [4]Bellanca *et al.*, 1997, n=13; [5]Webb and Kamber, 2000, n=28.

reefal microbialite, Webb and Kamber, 2000).

The limestones with higher REE concentrations (6.960 to 13.753 ppm) also exhibit distinct seawater-like REE+Y patterns. The observed seawater-like REE+Y pattern in these limestones mainly reflects the absorption of REE from contemporaneous seawaters with only minor contribution of REE from detrital materials (< 5% of local shale contamination). Hence, the ancient limestones deposited in the distal part of the basin having little detrital materials are suitable to understand the REE patterns of ancient shallow seawater and also they serve as a valuable seawater proxy.

CONCLUSIONS

The limestones of the Canova and El Caloso members have slight variations in major, trace and rare earth elements concentrations. Both negative and positive Ce anomalies and the observed variations in Ce and Ce anomalies in these limestones were controlled by scavenging process as well as detrital input. The observed positive Mn* values and low contents of U and authigenic U in the limestones of Canova and El Caloso members suggest that these limestones were deposited under oxic environment. The limestones possess low ΣREE contents, high Y/Ho ratios, low La_N/Yb_N ratios and seawater-like REE+Y patterns suggesting that the REE concentrations were mainly derived from seawater. Comparison of studied limestones with limestone from literature review show seawater patterns, La_N/Yb_N ratios falling in the range of average seawater indicate that the seawater was the REE source in the limestones. However, positive correlation of Al_2O_3 with ΣREE contents and Nd_N/Yb_N ratios suggests presence of minor contamination. These limestones were affected by minor shale contamination but still they retain their original seawater pattern. Our results indicate that the original seawater-like REE patterns remain unchanged in the limestones provided the contamination was minimal (<5%) and also they serve as a valuable seawater proxy.

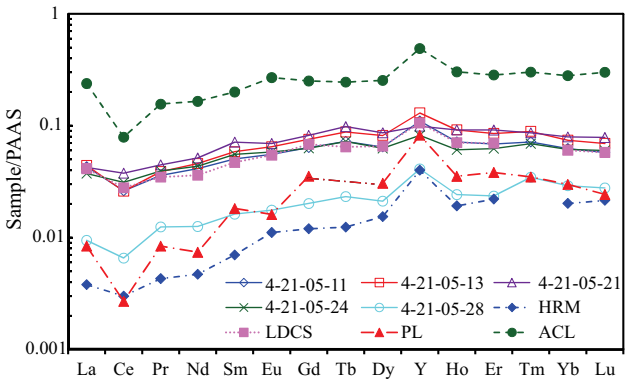

Figure 6. The limestones of Canova and El Caloso members are compared with limestones that exhibit seawater-like REE+Y pattern (Late Devonian carbonate sediments (LDCS), Nothdurft *et al.*, 2004; Permian Limestone (PL), Kawabe *et al.*, 1991; Albian-Cenomanian Limestone (ACL), Bellanca *et al.*, 1997; Holocene reefal microbialite (HRM), Webb and Kamber, 2000).

ACKNOWLEDGEMENTS

The first author would like to thank Dr. Thierry Calmus, ERNO, Instituto de Geologia, Universidad Nacional Autónoma de Mexico for his support and encouragement during this work. We acknowledge the support rendered by Universidad Nacional Autónoma de Mexico through PAPIIT Project No.IN121506-3. The field study of this work was partly supported by PAPIIT Project No. IN107803-3. We would like to express our gratefulness to Dr. Edgar Santoyo for his useful suggestions. We would like to thank Mr. Rufino Lozano-Santa Cruz (XRF analysis), Mrs. Elena Lounejeva and Dr. Juan Pablo Bernal (ICP-MS analysis) for their help in geochemical analyses. We would like to thank Mr. Pablo Peñaflor for powdering of limestone samples for geochemical studies. We also thank Dr. Teresa Pi I Puig, Instituto de Geología, Universidad Nacional Autónoma de México, México for her help in XRD analysis.

REFERENCES

Alibio, D.S., Nozaki, Y., 1999, Rare earth elements in seawater: Particle association, shale-normalisation, and Ce oxidation: Geochimica et Cosmochimica Acta, 63, 363-372.

Anderson, R., Bacon, M.P., Brewer., P.G., 1983, Removal of 230^{Th} and 234Pb at ocean margins: Earth and Planetary Science Letters, 66, 73-90.

Armstrong-Altrin, J.S., Verma, S.P., Madhavaraju, J., Lee, Y.I., Ramasamy, S., 2003, Geochemistry of Upper Miocene Kudankulam Limestones, Southern India: International Geological Review, 45, 16-26.

Barnes, U.C., Cochran, J.R., 1990, Uranium removal in oceanic sediments and the oceanic U balance: Earth and Planetary Science Letters, 97, 94-101.

Bau, M., 1996, Controls on fractionation of isovalent trace elements in magmatic and aqueous systems: Evidence from Y/Ho, Zr/Hf and lanthanide tetrad effect: Contribution to Mineralogy and Petrology, 123, 323-333.

Bau, M., Dulski, P., 1996, Distribution of yttrium and rare earth elements in the Penge and Kuruman iron formation, Transvaal Supergroup, South Africa: Precambrian Research, 79, 37-55.

Bellanca, A., Claps, M., Erba, E., Masetti, D., Neri, R., Premoli Silva, I., Venecia, F., 1996, Orbitally induced limestone/marlstone rhythms in the Albian-Cenomanian Cismon section (Venetian region, northern Italy): sedimentology, calcareous and siliceous plankton distribution, elemental and isotope geochemistry: Palaeogeography Palaeoclimatology Palaeoecology 126, 227-260.

Bellanca, A., Masetti, D., Neri, R.. 1997, Rare earth elements in limestone/marlstone couplets from the Albian-Cenomanian Cismon section (Venetian region, northern Italy): assessing REE sensitivity to environmental changes: Chemical Geology, 141, 141-152.

Bilodeau, W.L., Linberg, F.A., 1983, Early Cretaceous tectonics and sedimentation in southern Arizona, southwestern New Mexico, and northern Sonora, Mexico, *in* Reynolds, M.W., Dolly, E.D. (eds.), Mesozoic paleogeography of West-Central United States: Society of Economic Paleontologists and Mineralogists, Rocky Mountain Section, Rocky Mountain Paleogeography Symposium, 2, 173-188.

Bilodeau, W.L., Kluth, C.F., Vedder, L.K., 1987, Regional stratigraphic, sedimentologic, and tectonic relationships of the Glance Conglomerate in southeastern Arizona, *in* Dickinson, W.R., Klute, M.F. (eds.), Mesozoic rocks of southern Arizona adjacent areas: Arizona Geological Society Digest, 18, 229-256.

Biscaye, P. E., 1965, Mineralogy and sedimentation of recent deep sea clay in the Atlantic Ocean and adjacent seas and oceans: Bulletin Geological Society of America, 76, 803-832.

Bolhar, R., Kamber, B.S., Moorbath, S, Fedo, C.M., Whitehouse, M.J., 2004, Characterisation of early Archaean chemical sediments by trace element signatures: Earth and Planetary Science Letters, 222, 43-60.

Byrne, R.H., Liu, X., Schijf, J., 1996, The influence of phosphate coprecipitation on rare earth element distributions in natural waters: Geochimica et Cosmochimica Acta, 60, 3341-3346.

Cantu-Chapa, A., 1976, Nuevas localidades del Kimeridgiano y Titoniano in Chihuahua (Norte de Mexico): Revista del Instituto Mexicano del Petroleo, 7, 38-45.

Condie, K.C., 1991, Another look at rare earth elements in shales: Geochimica et Cosmochimica Acta, 55, 2527-2531.

De Baar, H.J.W., Bacon, M.P., Brewer, P.G., Bruland, K.W., 1985, Rare earth elements in the Pacific and Atantic oceans: Geochimica et Cosmochimica Acta, 49, 2561-2571.

De Baar, H.J.W., German, C.G., Elderfield, H., van Gaans, P., 1988, Rare earth elements distributions in anoxic waters of the Cariaco Trench: Geochimica et Cosmochimica Acta, 52, 1203-1219.

De Baar, H.J.W., Schijf, J., Byrne, R.H., 1991, Solution chemistry of the rare earth elements in seawater: European Journal of Solid State Inorganic Chemistry, 28, 357-373.

Dickinson, W.R., Klute, M.A., Swift, P.A., 1986, The Bisbee Basin and its bearing on late Mesozoic paleogeographic and paleotectonic relations between the Cordilleran and Carribean regions, *in* Abbott, P.L. (ed.), Cretaceous Stratigraphy: Western North America, Pacific Section (SEPM) Book, 46, 51-62.

Dickinson, W.R., Klute, M.A., Swift, P.A., 1989, Cretaceous strata of southern Arizona, *in* Jenney, J.P., Reynols, S.J. (eds.), Geologic Evolution of Arizona: Arizona Geological Society Digest, 17, 447-462.

Eggins, S.M., Woodhead, J.D., Kinsley, L.P.J., Mortimer, G.E., Sylvester, P., McCulloch, M.T., Hergt, J.M., Handler, M.R., 1997, A simple method for the precise determination of >=40 trace elements in geological samples by ICPMS using enriched isotope internal standardization: Chemical Geology, 134, 311-326.

Elderfield, H., 1988, The oceanic chemistry of the rare earth elements: Philosophical Transactions of the Royal Society of London, A325, 105-126.

Elderfield, H., Greaves, M.J., 1982, The rare earth elements in seawater: Nature, 296, 214-219.

Elderfield, H., Upstill-Goddard, R., Sholkovitz, E.R. 1990, The rare earth elements in rivers, estuaries and coastal seas and their significance to the composition of ocean waters: Geochimica et Cosmochimica Acta, 54, 971-991.

German, C.R., Elderfield, H. 1990, Application of Ce anomaly as a paleoredox indicator: the ground rules: Paleoceanography, 5, 823-833.

González-León, C.M., Scott, R.W., Loser, H., Lawton, T.F., Robert, E., Valencia, V.A., 2008, Upper Aptian-Lower Albian Mural Formation: stratigraphy, biostratigraphy and depositional cycles on the Sonoran shelf, northern Mexico: Cretaceous Research, 29, 249-266.

Govindaraju, K. 1994, Compilation of Working Values and Sample Description for 383 standard reference materials: Geostandards Newsletter, 18, 331.

Grandjean, P., Cappetta, H., Michard, A., Albarede, F., 1987, The assessment of REE patterns and $^{143}Nd/^{144}Nd$ ratios in fish remains: Earth and Planetary Science Letters, 84, 181-196.

Grandjean, P., Cappetta, H., Albarède, F., 1988, The REE and Nd of 40-70 Ma old fish debris from the West-African platform: Geophysical Research Letters, 15, 389-392.

Greaves, M.J., Elderfield, H., Sholkovitz, E.R. 1999, Aeolian sources of rare earth elements to the Western Pacific Ocean: Marine Chemistry, 68, 31-38.

Grim, R.E. 1968, Clay mineralogy: McGraw-Hill, New York, 600 pp.

Hardy, R., Tucker, M. 1988, X-ray powder diffraction of sediments, *in* Tucker, M. (ed.), Techniques in Sedimentology: Blackwell Scientific Publications, Oxford, 191-228.

Holser, W.T., 1997, Evaluation of the application of rare earth elements to paleoceanography: Palaeogeography, Palaeoclimatology, Palaeoecology, 132, 309-323.

Imai, N., Terashima, S., Itoh S., Ando, A., 1995, 1994 compilation of analytical data for minor and trace elements in seventeen GSJ geochemical reference samples, "Igneous rock series": Geostandards Newsletter, 19, 135-213.

Jacques-Ayala, C., 1995, Paleogeography and provenance of the Lower Cretaceous Bisbee Group in the Caborca-Santa Ana area, northwestern Sonora, *in* Jacques-Ayala, C., González-León, C.M., Roldan-Quintana, J. (eds.), Studies on the Mesozoic of Sonora and adjacent areas: Geological Society of America, Special Paper 301, 79-98.

Kamber, B.S., Webb, G.E., 2001, The geochemistry of late Archaean microbial carbonate: Implications for ocean chemistry and continental erosion history: Geochimica et Cosmochimica Acta, 65, 2509-2525.

Kawabe, I., Kitahara, Y., Naito, K., 1991, Non-chondritic yttrium/holmium ratio and lanthanide tetrad effect observed in pre-Cenozoic limestones: Geochemical Journal, 25, 31-44.

Klinkhammer, G.P., Elderfield, H., Hudson, A., 1983, Rare earth elements in seawater near hydrothermal vents: Nature, 305, 185-188.

Klinkhammer, G.P., Palmer, M.R., 1991, Uranium in the ocean, where it goes and why: Geochimica et Cosmochimica Acta, 55, 1799-1806.

Klute, M.A., 1991, Sedimentology, sandstone petrofacies, and tectonic

setting of the late Mesozoic Bisbee basin, southeastern Arizona: University of Arizona, unpublished Ph.D dissertation, 268 pp.

Krauskopf, K.B., 1979, Introduction to Geochemistry: Tokyo, McGraw-Hill Kogakusha, 617 pp.

Lachance, G.R., Traill, R.J., 1966, A practical solution to the matrix problem in X-ray analysis, I. Method: Canadian Spectroscopy, 11, 43-48.

Lawrence, M.G., Kamber, B.S. 2006, The behaviour of the rare earth elements during estuarine mixing - revisited: Marine Chemistry, 100, 147-161.

Lawton, T.F., González-León, C.M., Lucas, S.G., Scott, R.W., 2004, Stratigraphy and sedimentology of the upper Aptian-upper Albian Mural Limestone (Bisbee Group) in northern Sonora, Mexico: Cretaceous Research, 25, 43-60.

Liu, Y.G., Miah, M.R.U., Schmitt, R.A., 1988, Cerium: a chemical tracer for paleo-oceanic redox conditions: Geochimica et Cosmochimica Acta, 52, 1361-1371.

Machhour, L., Philip, J., Oudin, J.L., 1994, Formation of laminate deposits in anaerobic-dysaerobic marine environments: Marine Geology, 117, 287-302.

Mack, G.H., Kolins, W.B., Galemore, J.A., 1986, Lower Cretaceous stratigraphy, depositional environments, and sediment dispersal in southwestern New Mexico: American Journal of Science 286, 309-331.

MacLeod, K.G., Irving, A.J., 1996, Correlation of cerium anomalies with indicators of paleoenvironment: Journal of Sedimentary Research, 66, 948-955.

Madhavaraju, J., Lee, Y.I., 2009, Geochemistry of the Dalmiapuram Formation of the Uttatur Group (Early Cretaceous), Cauvery Basin, southeastern India: Implications on provenance and paleo-redox conditions: Revista Mexicana de Ciencias Geológicas, 26, 380-394.

Madhavaraju, J., Ramasamy, S. 1999, Rare earth elements in limestones of Kallankurichchi Formation of Ariyalur Group, Tiruchirapalli Cretaceous, Tamil Nadu: Journal of the Geological Society of India, 54, 291-301.

Madhavaraju, J., Löser, H., González-León, C.M., 2008**,** Geochemistry of clastic rocks of Mural Formation (Aptian-Albian), Northern Sonora, Mexico, *in* XVIII Congreso Nacional de Geoquímica, Hermosillo, Sonora: Departamento de Geologia, Universidad de Sonora y ERNO-Instituto de Geologia, Universidad Nacional Autónoma de México, p.59.

Madhavaraju, J., González-León, C.M., Lee, Y.I., Armstrong-Altrin, J.S., Reyes-Campero, L.M., 2010, Geochemistry of the Mural Formation (Aptian-Albian) of the Bisbee Group, Northern Sonora, Mexico: Cretaceous Research, 31, 400-414

Masuzawa, T., Koyama, M., 1989, Settling particles with positive Ce anomalies from the Japan Sea: Geophysical Research Letters, 16, 503-506.

Muller, G., 1967, Methods in Sedimentary Petrology: New York, Hefner Publishing Company, 281 pp.

Nagarajan, R., Madhavaraju, J., Armstron-Altrin, J.S., Nagendra, R., 2011, Geochemistry of Neoproterozoic limestones of the Shahabad Formation, Bhima Basin, Karnataka, southern India: Geosciences Journal, 15, 9-25.

Nath, B.N., Bau, M., Ramlingeswara Rao, B., Rao, Ch.M., 1997, Trace and rare earth elemental variation in Arabian Sea sediments through a transect across the oxygen minimum zone: Geochimica et Cosmochimica Acta, 61, 2375-2388.

Nothdurft, L.D., Webb, G.E., Kamber, B.S., 2004, Rare earth element geochemistry of Late Devonian reefal carbonates, Canning Basin, Western Australia: Confirmation of seawater REE proxy in ancient limestones: Geochimica et Cosmochimica Acta, 68, 263-283.

Nozaki, Y., Alibio, D.S., 2003, Importance of vertical geochemical processes in controlling the oceanic profiles of dissolved rare earth elements in northeastern Indian Ocean: Earth and Planetary Science Letters, 205, 155-172.

Nozaki, Y., Horibe, Y., Tsubota, H., 1981, The water column distribution of thorium isotopes in the western North Pacific: Earth and Planetary Science Letters, 54, 203-216.

Piepgras, D.J., Jacobsen, S.B., 1992, The behaviour of rare earth elements in seawater: precise determination of variations in the North Pacific water column: Geochimica et Cosmochimica Acta, 56, 1851-1862.

Piper, D.Z., 1974, Rare earth elements in the sedimentary cycle, a summary: Chemical Geology, 14, 285-304.

Ransome, F.L., 1904, The geology and ore deposits of the Bisbee quadrangle Arizona: U.S. Geological Survey, Professional Paper, 21, 167 pp.

Santoyo, E., Verma, S.P., 2003, Determination of lanthanides in synthetic standards by reversed-phase high performance liquid chromatography with the aid of a weighted least-squares regression model: estimation of method sensitivities and detection limits: Journal of Chromatography, A 997, 171-182.

Sarkar, A., Bhattacharya, S.K., Sarin, M.M., 1993, Geochemical evidence for anoxic deep sea water in the Arabian Sea during the last glaciations: Geochimica et Cosmochimica Acta, 57, 1009-1016.

Scott, R.W., 1987, Stratigraphy and correlation of the Cretaceous Mural Limestone, Arizona and Sonora, *in* Dickinson, W.R., Klute, M.F. (eds.), Mesozoic rocks of Southern Arizona adjacent areas: Arizona Geological Society Digest, 18, 327-334.

Shaw, H.F., Wasserburg, G.J., 1985, Sm-Nd in marine carbonates and phosphates: Implications for Nd isotopes in seawater and crustal ages: Geochimica et Cosmochimica Acta, 49, 503-518.

Shields, G.A., Webb, G.E., 2004, Has the REE composition of seawater changed over geologic time: Chemical Geology, 204, 103-107.

Sholkovitz, E.R., 1990, Rare earth elements in marine sediments and geochemical standards: Chemical Geology, 88, 333-347.

Sholkovitz, E.R., Landing, W.M., Lewis, B.L., 1994, Ocean particle chemistry: the fractionation of rare earth elements between suspended particles and seawater: Geochimica et Cosmochimica Acta, 58, 1567-1579.

Somayajulu, B.L.K., Yadav, D.N., Sarin, M.M., 1994, Recent sedimentary records from the Arabian sea: Proceeding of Indian Academy of Science (Earth and Planetary Science), 103, 315-327.

Taylor, S.R., McLennan, S.M., 1985, The Continental crust: its composition and evolution: Oxford, Blackwell, 349 pp.

Turekian, K.K., Wedepohl, K.H. 1961, Distribution of elements in some major units of earth's crust: Geological Society of America Bulletin, 72, 175-192.

Van Kranendonk, M., Webb, G.E., Kamber, B.S., 2003, Geological and trace evidence for a marine sedimentary environment of deposition and biogenicity of 3.45 Ga stromatolitic carbonates in the Pilbara Craton, and support for a reducing Archaean ocean: Geobiology, 1, 91-108.

Verma, S.P., 2005, Estadística Básica para el Manejo de Datos Experimentales: Aplicación en la Geoquímica (Geoquimiometría): Mexico, D.F., Universidad Nacional Autónoma de México, 186 pp.

Verma, S.P., Santoyo, E., 2005, Is odd-even effect reflected in detection limits?: Accreditation and Quality Assurance, 10, 144-148.

Verma, S.P., Santoyo, E., Velasco-Tapia, F., 2002, Statistical evaluation of analytical methods for the determination of rare-earth elements in geological materials and implications for detection limits: International Geology Review, 44, 287-335.

Warzeski, E.R., 1983, Facies patterns and diagenesis of a Lower Cretaceous carbonate shelf: northeastern Sonora and southeastern Arizona: Binghamton, State University New York, Ph.D. thesis, 401 pp.

Warzeski, E.R., 1987, Revised stratigraphy of the Mural Limestone: a Lower Cretaceous carbonate shelf in Arizona and Sonora, *in* Dickinson, W.R., Klute, M.F. (eds.), Mesozoic Rocks of Southern Arizona Adjacent Areas: Arizona Geological Society Digest, 18, 335-363.

Webb, G.E., Kamber, B.S., 2000, Rare earth elements in Holocene reefal microbialites: A new shallow seawater proxy: Geochimica et Cosmochimica Acta, 64, 1557-1565.

Wedepohl, K.H., 1978, Manganese: abundance in common sediments and sedimentary rocks: Berlin, Springer, Handbook of Geochemistry, 1-17.

Whittaker, S.G., Kyser, T.K., 1993, Variations in the neodymium and

strontium isotopic composition and REE content of molluscan shells from the Cretaceous Western Interior Seaway: Geochimica et Cosmochimica Acta, 57, 4003-4014.

Wignall, P.B., Myers, K.J., 1988, Interpreting the benthic oxygen levels in mudrocks, a new approach: Geology, 16, 452-455.

Wright, J., Seymour, R. S., and Shaw, H. F., 1984, REE and neodymium isotopes in conodont apatite. Variation with geological age and depositional environment: Geological Society of America Special Paper, 196, 325-340.

Wright, J., Schrader, H., Holser, W.T., 1987, Paleoredox variations in ancient oceans recorded by rare earth elements in fossil apatite: Geochimica et Cosmochimica Acta, 60, 4631-4644.

Zhang, J., Nozaki, Y., 1996, Rare earth elements and yttrium in seawater: ICP-MS determinations in the East Caroline, Coral Sea, and South Fiji basins of the western South Pacific Ocean: Geochimica et Cosmochimica Acta, 60, 4631-4644.

Manuscript received: June 21, 2011
Corrected manuscript received: February 15, 2012
Manuscript accepted: March 7, 2012